Applied Catalysis B: Environmental 142–143 (2013) 8–14

Contents lists available at SciVerse ScienceDirect

Applied Catalysis B: Environmental

journal homepage: www.elsevier.com/locate/apcatb

Effect of platinum dispersion on the catalytic activity of Pt/Al_2O_3 for the oxidation of carbon monoxide and propene

Masaaki Haneda*, Tokuya Watanabe, Naoto Kamiuchi[1], Masakuni Ozawa[1]

Advanced Ceramics Research Center, Nagoya Institute of Technology, 10-6-29 Asahigaoka, Tajimi, Gifu 507-0071, Japan

ARTICLE INFO

Article history:
Received 29 November 2012
Received in revised form 23 April 2013
Accepted 26 April 2013
Available online 4 May 2013

Keywords:
Platinum dispersion
CO oxidation
C_3H_6 oxidation
Pt/Al_2O_3
In situ FT-IR spectroscopy

ABSTRACT

Effect of Pt dispersion on the catalytic performance of Pt/Al_2O_3 for CO and C_3H_6 oxidation was investigated. The intrinsic activity, expressed in terms of turnover frequency (TOF), for CO oxidation on Pt/Al_2O_3 catalysts was found to be almost identical irrespective of Pt dispersion. Pt dispersion is the most important factor to determine the CO oxidation activity. On the other hand, the TOF values for C_3H_6 oxidation on Pt/Al_2O_3 catalysts were found to increase with increasing the Pt dispersion to 0.20 and then remain almost invariable above $D_{Pt} = 0.20$. *In situ* FT-IR spectroscopy suggested that acrylate species participates as a reaction intermediate in C_3H_6 oxidation on Pt/Al_2O_3 and the formation and reaction behavior of the acrylate species is different depending on the Pt dispersion. The acrylate species formed on Pt/Al_2O_3 with higher Pt dispersion can readily react with oxygen to form CO_2. On the other hand, the reaction of acrylate species is the slow step in the reaction over Pt/Al_2O_3 with $D_{Pt} = 0.07$. Low TOF values on Pt/Al_2O_3 with lower Pt dispersion were considered to be due to the inhibition of catalytically active site by accumulation of acrylate species.

1. Introduction

Supported noble metal (PGM: Pt, Rh and Pd) catalysts are widely used in the practical application, such as automotive emission control [1,2], catalytic combustion [3,4], steam reforming [5] and various hydrogenation reactions [6,7]. The catalytic reaction predominantly occurs on the catalytic surface. Therefore, the particle size of the noble metal is one of the important factors to determine the catalytic activity. On the other hand, growth of noble metal particles and attendant loss of surface area are often observed under operation conditions, leading to deactivation of the supported noble metal catalysts. In particular, automotive catalysts, typified by the three-way catalyst which simultaneously and efficiently reduces NO and oxidizes CO and hydrocarbons, are exposed to high temperature exhaust gases (~1000 °C), so that sintering of the noble metal particles is one of the major reasons for the catalyst deterioration. Keeping the noble metal in highly dispersed state even under operation conditions seems to be a key technology to develop highly active catalysts.

The optimum particle size of the noble metal is, however, suspected to be different depending on the type of catalytic reactions. Because a catalyst surface is not uniform and varies with particle size, in many cases, the reaction rate normalized by the number of active sites, expressed as turnover frequency (TOF), cannot be merely summarized as a function of particle size. For example, Haruta [8] reported that the TOFs of CO oxidation over Au/TiO_2 sharply increased with a decrease in the diameter of Au particles from 4 nm. On the other hand, Prashar et al. [9] revealed that Pt catalysts supported on SBA-15 shows steady TOF of CO oxidation in the Pt particle size from 3 to 10 nm, suggesting structure insensitivity. The dependence of particle size on CO oxidation reaction seems to be different depending on the kinds of noble metal. As for the total oxidation of hydrocarbon, Gandhi and Shelef [10] reported that alkane oxidation on automotive catalysts with highly dispersed noble metals is relatively slow and the catalyst including too large particles also becomes less efficient due to a decrease of the fraction of surface atoms. This suggests the presence of an optimum particle size. The optimum particles size may be determined by the surface properties of noble metals including morphology, crystal face and electron density. On the other hand, Gololobov et al. [11] reported that the specific activity of 0.8 wt% Pt/Al_2O_3 for the total oxidation of C_1–C_6 n-alkanes increases with an increase in the Pt particle size. The effect of particle size on the activity of supported Pt catalysts also seems to be different depending on the kinds of hydrocarbons employed.

In the present study, we have prepared Pt/Al_2O_3 with different Pt dispersion by controlling the preparation conditions in order to

* Corresponding author. Tel.: +81 572 27 6811; fax: +81 572 27 6812.
E-mail address: haneda.masaaki@nitech.ac.jp (M. Haneda).
[1] Present address: EcoTopia Science Institute, Nagoya University, Furo-cho, Chikusa-ku, Nagoya 464-8603, Japan.

0926-3373/$ – see front matter © 2013 Elsevier B.V. All rights reserved.
http://dx.doi.org/10.1016/j.apcatb.2013.04.055

Table 1
Dispersion and averaged particle size of platinum supported on alumina.

Calcination conditions	Amount of CO chemisorption (mol g_{cat}^{-1})	Pt dispersion (D_{Pt})	Averaged particle size of Pt (nm)	
			CO chemisorption	TEM
500 °C, 3 h	4.15×10^{-5}	0.81	1.8	<5
600 °C, 1 h	3.02×10^{-5}	0.59	2.5	
600 °C, 10 h	2.36×10^{-5}	0.46	3.2	
700 °C, 0.1 h	1.85×10^{-5}	0.36	4.1	20
650 °C, 1 h	1.08×10^{-5}	0.21	7.0	22
650 °C, 5 h	6.15×10^{-6}	0.12	12	30
700 °C, 5 h	3.59×10^{-6}	0.07	21	

investigate the effect of Pt dispersion state on oxidation reactions. We examined the effect of Pt dispersion on the oxidation reactions of CO and C_3H_6 as reactant because both reactants are major pollutants in vehicle exhaust. In the course of this study, we have found that the TOF of CO oxidation on Pt/Al_2O_3 catalysts is almost identical irrespective of Pt dispersion, while the TOF of C_3H_6 oxidation on Pt/Al_2O_3 catalysts increase with increasing the Pt dispersion. Therefore, a systematic *in situ* FT-IR study of the formation and reaction of adsorbed species in C_3H_6 oxidation was also carried out to clarify the effect of Pt dispersion.

2. Experimental

1 wt% Pt/Al_2O_3 was prepared by impregnation of Al_2O_3 (Sumitomo Chemicals, AKP-G015, 156 $m^2\,g^{-1}$) with a solution of $Pt(NO_2)_2(NH_3)_2$, followed by drying and calcination at 500 °C for 3 h in air. The sample was further calcined at 600, 650 and 700 °C for several hours to obtain different Pt dispersions in air. Heating rate for calcination was fixed at 10 °C min^{-1}.

The amount of chemisorbed CO was measured with a pulse method. The sample was first reduced with H_2 at 400 °C for 1 h and then cooled to room temperature in flowing He. Several pulses of CO were introduced into the sample until no more adsorption was observed. The Pt dispersion, expressed in terms of $CO_{chemisorbed}/Pt_{total}$ ratio, was calculated by assuming a CO to surface Pt atom ratio of 1:1 [12,13]. FT-IR spectra of adsorbed CO species were taken with a JASCO FT/IR 4200 spectrometer at a resolution of 4 cm^{-1} under a static condition. Prior to each experiment, a self-supporting sample disk (14 mg cm^{-2}) was placed in an IR cell with CaF_2 windows, pretreated with hydrogen at 13.3 kPa for 1 h, and then evacuated at 400 °C for 1 h. The background spectrum of the treated surface was measured for spectral correction at room temperature. Observation of surface species was carried out after introduction of CO at 6.67 kPa at room temperature. Direct observation of Pt particles by TEM was performed with a JEM-2100 (JEOL) operating at an acceleration voltage of 200 kV.

The catalytic activity for CO and C_3H_6 oxidation was evaluated using a fixed-bed continuous flow reactor. A reaction gas mixture containing either CO (0.5%) or C_3H_6 (600 ppm) as a reactant and O_2 (1%) diluted in He as the balance gas was fed through a catalyst (30 mg), pretreated *in situ* in a flow of 5% H_2/He at 400 °C for 1 h, at a rate of 50 $cm^3\,min^{-1}$ (SV = *ca.* 50,000 h^{-1}). The activity was measured while decreasing the temperature from 400 to 50 °C in steps of 20 °C, and the steady-state catalytic activity was measured at each temperature. The effluent gas was analyzed with the use of on-line gas chromatograph equipped with TCD and FID as a detector (Shimadzu GC-2014ATTF). In case of C_3H_6 oxidation, no formation of CO and other hydrocarbons as product was observed. The catalytic activity was evaluated in terms of CO or C_3H_6 conversion to CO_2. In a series of experiments, TOFs for each CO and C_3H_6 oxidation reactions were calculated with the reaction rate for CO_2 formation measured under nearly differential conditions giving CO and C_3H_6 conversions <20% as follows:

TOF(mol-CO_2 min^{-1} Pt-atoms^{-1}) = (reaction rate for CO_2 formation (mol-CO_2 min^{-1} g-cat^{-1}))/(number of surface Pt atoms estimated by CO chemisorption (Pt-atoms g-cat^{-1})).

In situ FT-IR spectra were recorded with a Nicolet 6700 FT-IR spectrometer, accumulating 64 scans at a resolution of 4 cm^{-1}. Prior to each experiment, a self-supporting sample disk (14 mg cm^{-2}) placed in an IR cell with CaF_2 windows was pretreated in a flow of 5% H_2/He at 400 °C. Observation of surface species was carried out after introducing a reaction gas comprised of C_3H_6 (600 ppm), O_2 (1%) and Ar (0.5%) with the balance of He at a flow rate of 30 $cm^3\,min^{-1}$. The effluent gas was analyzed by on-line quadrupole mass spectrometer (PFEFFER OminiStar).

3. Results and discussion

3.1. Pt dispersion

Table 1 summarizes the amount of CO chemisorption and Pt dispersion (D_{Pt}) in Pt/Al_2O_3. When Pt/Al_2O_3 was calcined at 500–700 °C for various hours, the Pt/Al_2O_3 catalysts with Pt dispersion ranging from 0.81 to 0.07 were obtained. A slight decrease in BET surface area of Pt/Al_2O_3 from 156 to 133 $m^2\,g^{-1}$ was observed after calcination at 700 °C for 5 h (results not shown).

Fig. 1 shows TEM images of Pt/Al_2O_3 calcined at 700 °C for 0.1 h and at 650 °C for 5 h. When Pt/Al_2O_3 was calcined at 700 °C for 0.1 h (Fig. 1(A)), Pt particles were found to be dispersed with a size of 15–20 nm over the surface of Al_2O_3. On the other hand, an aggregation of Pt particles was observed for Pt/Al_2O_3 calcined at 650 °C for 5 h (Fig. 1(B)). The size of Pt particles was found to be 25–30 nm. As summarized in Table 1, averaged Pt particle size estimated by TEM was quite larger than that estimated from the amount of CO chemisorption. This is probably due to the presence of very small Pt particles, which cannot be observed by TEM analysis.

3.2. CO oxidation reaction

Fig. 2 shows the catalytic activity of Pt/Al_2O_3 with different Pt dispersion for CO oxidation. Obviously, the highest CO oxidation activity was achieved for Pt/Al_2O_3 with D_{Pt} = 0.81, which is the highest Pt dispersion. CO oxidation activity of Pt/Al_2O_3 was monotonously decreased with decreasing Pt dispersion. Fig. 3 shows the change in TOF of CO oxidation at 120 and 160 °C at which nearly differential conditions were attained as a function of Pt dispersion, where TOF expressed as moles of CO oxidized to CO_2 per mole of surface Pt atoms per minute was calculated. It appears that

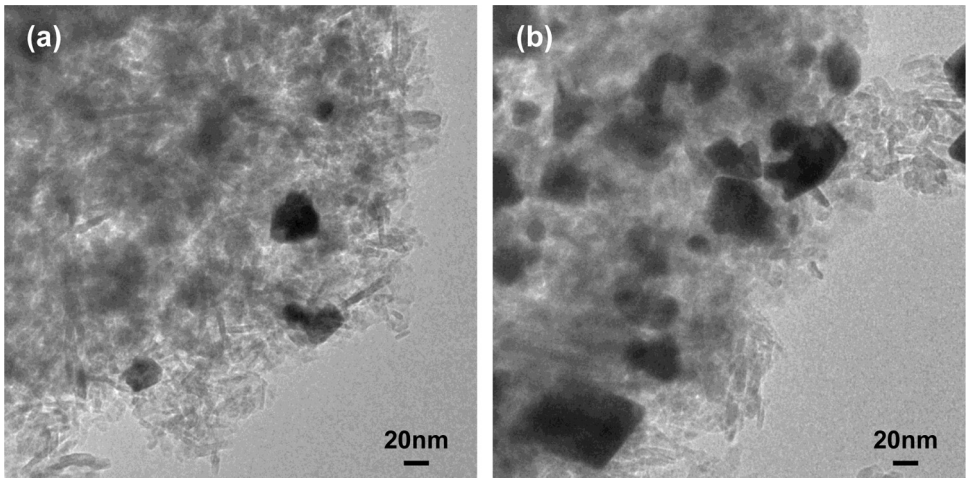

Fig. 1. TEM images of (A) Pt/Al_2O_3 calcined at 700 °C for 0.1 h (D_{Pt} = 0.36) and (B) at 650 °C for 5 h (D_{Pt} = 0.12).

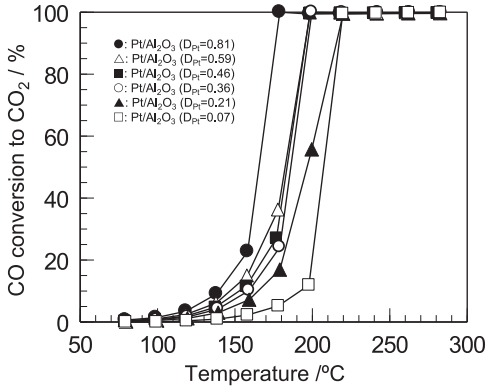

Fig. 2. Activity of Pt/Al_2O_3 with different Pt dispersion for CO oxidation. Conditions: CO = 0.5%, O_2 = 1%, He balance, catalyst weight = 30 mg, total flow rate = 50 cm^3 min^{-1}. (●) D_{Pt} = 0.81, (△) D_{Pt} = 0.59, (■) D_{Pt} = 0.46, (○) D_{Pt} = 0.36, (▲) D_{Pt} = 0.21 and (□) D_{Pt} = 0.07.

the TOF at 120 and 160 °C was almost identical in the entire range of Pt dispersion, suggesting "structure–insensitive reaction" over Pt/Al_2O_3. This is in agreement with the results obtained on Pt/SiO_2 [8] and Pt/SBA-15 [9] reported so far. This would be explained by the consideration that CO oxidation proceeds predominantly on Pt sites and the surface electronic state of Pt particles is not altered by changing the size of Pt particles.

In order to estimate the surface electronic state of Pt supported on Al_2O_3, FT-IR spectra for CO species adsorbed on Pt/Al_2O_3 with different Pt dispersion were measured. As seen in Fig. 4(a), exposure of CO to Pt/Al_2O_3 with D_{Pt} = 0.81 gave a strong IR band at 2070 cm^{-1} due to CO species linearly adsorbed on Pt° sites [14–16]. Its band intensity decreased with decreasing Pt dispersion. An appearance of overlapped IR band at 2095 cm^{-1}, which is ascribed to linear CO species adsorbed on different Pt sites, was also observed for Pt/Al_2O_3 with Pt dispersion lower than 0.21. Fig. 5 shows deconvolution spectra of CO species adsorbed on Pt/Al_2O_3 with D_{Pt} = 0.46 and 0.12, as typical results. As summarized the results of peak deconvolution in Table 2, in addition to IR bands at *ca.* 2095 and 2070 cm^{-1}, broad IR band at *ca.* 2045 cm^{-1} was detected on each of different samples, suggesting the presence of three different Pt sites depending on the Pt dispersion. It should be noted that no significant shift of IR bands at 2095, 2070 and 2045 cm^{-1} was observed as

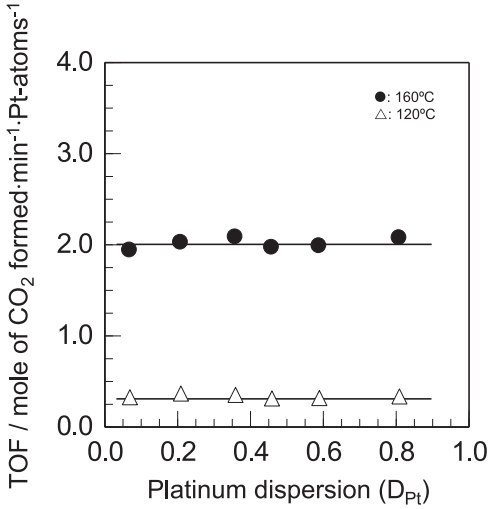

Fig. 3. Change in TOF of CO oxidation at 120 (△) and 160 °C (●) on Pt/Al_2O_3 as a function of platinum dispersion.

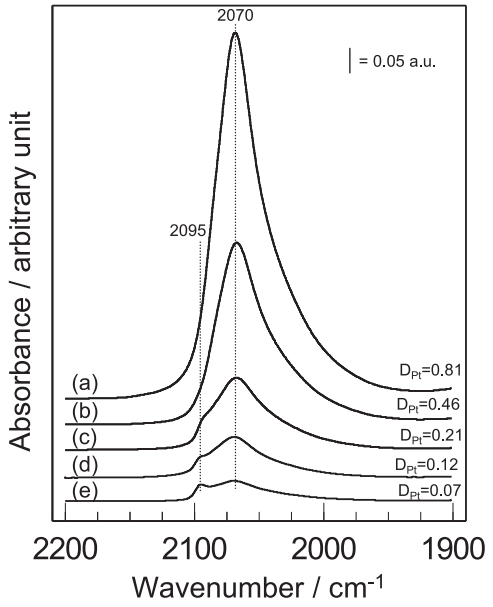

Fig. 4. FT-IR difference spectra of adsorbed CO species remaining on Pt/Al_2O_3 with different platinum dispersion after evacuation at room temperature. (a) D_{Pt} = 0.81, (b) D_{Pt} = 0.46, (c) D_{Pt} = 0.21, (d) D_{Pt} = 0.12 and (e) D_{Pt} = 0.07.

Table 2
Wavenumbers (cm^{-1}) of CO species adsorbed on Pt/Al_2O_3 and peak area of each IR band estimated from peak deconvolution.

Catalyst	Wavenumber (cm^{-1})			Peak area (a.u. cm^{-1})		
Pt/Al_2O_3				(2045 cm^{-1})	(2070 cm^{-1})	(2095 cm^{-1})
D_{Pt} = 0.81	2045	2070		17.9	17.0	
D_{Pt} = 0.46	2045	2069		10.6	8.05	
D_{Pt} = 0.21	2039	2069	2093	3.28	4.15	0.28
D_{Pt} = 0.12	2042	2071	2095	1.98	2.36	0.14
D_{Pt} = 0.07	2042	2072	2095	1.05	1.17	0.18

Pt dispersion was changed, suggesting that the surface electronic state of Pt particles is almost identical irrespective of Pt dispersion. Therefore, the fact that almost steady TOF was obtained for CO oxidation on Pt/Al_2O_3 (Fig. 3) would be explained by the identical surface electronic state of Pt particles as catalytically active sites.

Greenler et al. [17] measured IR spectra of CO species adsorbe on Pt/SiO_2 with different Pt particle size and observed three IR bands at 2081, 2070 and 2063 cm^{-1} on each of different samples. From the comparison of IR spectra observed for CO species adsorbed on three extended-crystal surface of Pt (a (1 1 1) crystal, a crystal with (1 1 1) terraces and (1 0 0) steps, and a crystal with (1 1 1) terraces and kinked steps), they assigned the three IR bands at 2081, 2070 and 2063 cm^{-1} to CO species linearly bound to face, corner and edge Pt atoms, respectively. Similar IR assignments were also reported by single crystal studies [18–20]. Taking into account the facts that the intensity of IR bands at *ca.* 2070 and 2045 cm^{-1} decreased with decreasing Pt dispersion and the IR band at *ca.* 2095 cm^{-1} was detected on Pt/Al_2O_3 with low Pt dispersion (Table 2), the IR bands at *ca.* 2095, 2070 and 2045 cm^{-1} would be assigned to CO species linearly bound to face, corner and edge Pt atoms, respectively. Since the TOF at 120 and 160 °C was almost identical in the entire range of Pt dispersion (Fig. 3), all the Pt atoms located at face, corner and edge sites would be the catalytically active sites for CO oxidation on supported Pt catalysts, although further detail experiments are necessary.

Thus, CO oxidation was found to be "structure–insensitive reaction" over Pt/Al_2O_3. Since FT-IR spectroscopy following CO adsorption revealed that the surface electron state of Pt supported on Al_2O_3 is almost identical irrespective of Pt dispersion (Fig. 4), the most important factor is the active site of Pt, which number is determined by the dispersion on support.

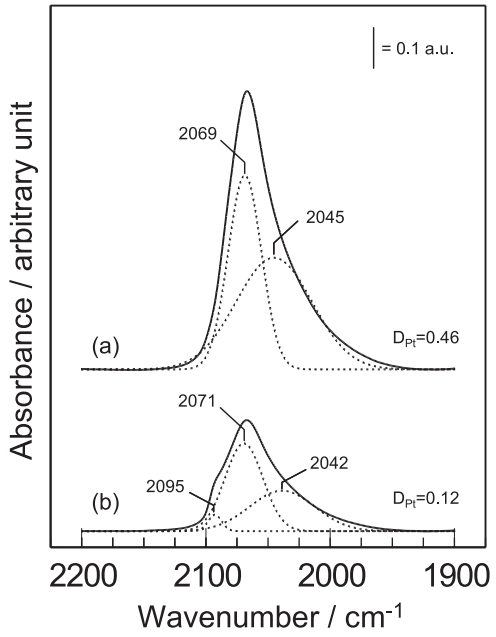

Fig. 5. Deconvolution spectra for CO species adsorbed on Pt/Al_2O_3 with different platinum dispersion. (a) D_{Pt} = 0.46 and (b) D_{Pt} = 0.12.

3.3. C_3H_6 oxidation reaction

3.3.1. Catalytic activity

Effect of Pt dispersion on the catalytic activity of Pt/Al_2O_3 for C_3H_6 oxidation was also investigated. As shown in Fig. 6, the conversion efficiency of C_3H_6 on Pt/Al_2O_3 was monotonously decreased with decreasing Pt dispersion from 0.81 to 0.07, indicating that small Pt particles seem to be highly active for C_3H_6 oxidation. This tendency is similar with that for CO oxidation, so that higher dispersion improves the catalytic oxidation performance as described before. C_3H_6 oxidation is also suspected to be "structure–insensitive reaction", if Pt surface participates as the catalytically active sites. In order to examine the structure sensitivity for C_3H_6 oxidation, the TOF on Pt/Al_2O_3 at 140 and 160 °C was estimated on the basis of mole of surface Pt atoms. As can be seen in Fig. 7, the TOF was found to be strongly dependent on the Pt dispersion in the region of low dispersion. The TOF values increased with increasing the Pt dispersion to 0.20, and then remained almost invariable above D_{Pt} = 0.20. This clearly suggests that C_3H_6 oxidation is "structure–sensitive reaction" on Pt/Al_2O_3.

Effect of Pt particle size on the catalytic activity for the total oxidation of alkane and alkene has been extensively studied so far. The observed dependencies of TOF on the Pt particle size are often different depending on the type of hydrocarbons and support oxide for Pt. Gololobov et al. [12] reported that the specific activity of 0.8 wt% Pt/Al_2O_3 for the total oxidation of C_1–C_6 n-alkanes increases with an increase in the Pt particle size from 1 to 3–4 nm and then further coarsening of the particles insignificantly changes the specific activity. They explained the high specific activity of Pt/Al_2O_3 with large Pt particles by the presence of crystallographic planes in which the Pt atoms are coordinatively less unsaturated. Garetto and Apesteguía [21] reported that the turnover rates on Pt/Al_2O_3 for cyclopentene oxidation increase drastically with increasing Pt

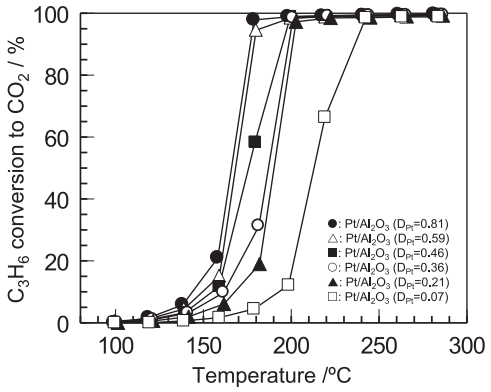

Fig. 6. Activity of Pt/Al_2O_3 with different Pt dispersion for C_3H_6 oxidation. Conditions: C_3H_6 = 600 ppm, O_2 = 1%, He balance, catalyst weight = 30 mg, total flow rate = 50 cm^3 min^{-1}. (●) D_{Pt} = 0.81, (△) D_{Pt} = 0.59, (■) D_{Pt} = 0.46, (○) D_{Pt} = 0.36, (▲) D_{Pt} = 0.21 and (□) D_{Pt} = 0.07.

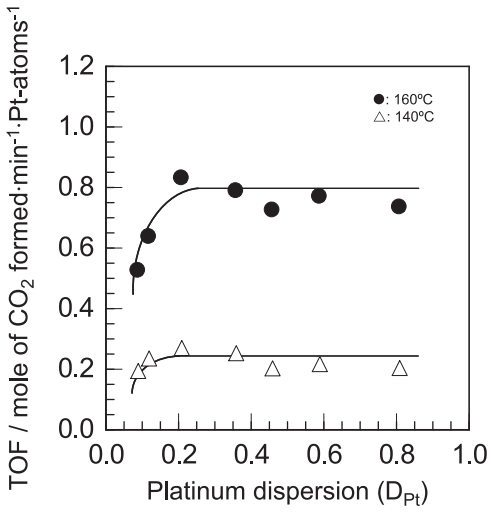

Fig. 7. Change in TOF of C_3H_6 oxidation at 140 (△) and 160 °C (●) on Pt/Al_2O_3 as a function of platinum dispersion.

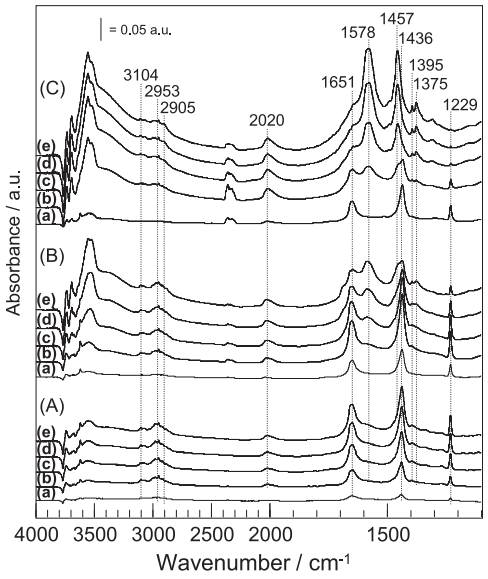

Fig. 8. Change of FT-IR spectra of adsorbed species formed during C_3H_6 oxidation after introducing the reaction gas over Pt/Al_2O_3 with D_{Pt} = 0.21 at (A) 100 °C, (B) 150 °C and (C) 200 °C for (a) 1 min, (b) 3 min, (c) 10 min, (d) 20 min and (e) 30 min. Reaction conditions: C_3H_6 = 600 ppm, O_2 = 1%, Ar = 0.5%, He balance, total flow rate = 30 cm^3 min^{-1}.

particle size. On the basis of reaction mechanism of cyclopentene oxidation in which cyclopentene is oxidized on metallic Pt active sites *via* a surface redox mechanism, they proposed the importance of the density of reactive Pt–O species, which increases with increasing Pt particle size. Similar dependencies of the turnover rates on noble metal particle size were also reported for n-pentane oxidation on Pt/Al_2O_3 [22] and Pd/Al_2O_3 [23], C_3H_8 oxidation on Pt/Al_2O_3 [24] and C_3H_6 oxidation over Pt/Al_2O_3 [24–26].

In the present study, FT-IR spectroscopy following CO adsorption (Fig. 4) revealed the presence of Pt atoms located at face, corner and edge sites depending on Pt particle size, where the presence of face Pt atoms was recognized on large Pt particles. Since Pt/Al_2O_3 with low Pt dispersion gave low TOF values for C_3H_6 oxidation (Fig. 7), Pt atoms located at face sites do not seem to participate in the reaction as active sites. Pt atoms located at corner and edge sites may act as active sites for C_3H_6 oxidation. On the other hand, on the basis of *in situ* FT-IR spectroscopy, we have recently proposed the participation of the Pt–Al_2O_3 interface as catalytically active sites in the total oxidation of hydrocarbon mixture (n-decane + 1-methylnaphthalene) [27,28]. In the present study, *in situ* FT-IR studies were also performed next to investigate the structure sensitivity of C_3H_6 oxidation on Pt/Al_2O_3 in details.

3.3.2. *In situ FT-IR spectroscopy*

Since no information on the formation and reaction behavior of intermediate species in the total oxidation of hydrocarbon mixture on Pt/Al_2O_3 was obtained in the FT-IR spectra recorded under a steady-state condition [28], we measured the change in the FT-IR spectra of the adsorbed species with reaction time on Pt/Al_2O_3 with different Pt dispersion at 100–200 °C after introducing the reaction gas. Fig. 8 shows the change in the FT-IR spectra measured for Pt/Al_2O_3 with D_{Pt} = 0.21. As seen in Fig. 8(A), weak but distinct IR bands were observed at 1651, 1436 and 1229 cm^{-1} in the first 1 min at the reaction temperature of 100 °C. These bands increased with reaction time up to 30 min. According to literature [29–31], the IR bands at 1651, 1436 and 1229 cm^{-1} can be assigned to ν(C═O), ν(COO) and ν(C—O) of the acrylate species, respectively. When the reaction was carried out at 150 °C (Fig. 8(B)), the IR bands due to acrylate species increased first with reaction time up to 10 min, and then decreased with time on stream. In addition, an appearance of new IR bands at 1578 and 1457 cm^{-1} and 1395 and 1375 cm^{-1} of which the former two bands can be assigned to carbonate and/or carboxylate species [29] while the latter two bands to formate species [32,33] was also observed after starting to decrease in the acrylate species, suggesting that these species are the products for the reaction of acrylate species with oxygen. Since the amount of CO species adsorbed on Pt, which was recognized by appearance of the IR band at 2020 cm^{-1}, increased with time on stream, CO is also suspected to be the product for the reaction of acrylate species with oxygen. The consumption of acrylate species and the formation of carbonate and/or carboxylate, formate and CO species were remarkably observed at 200 °C as seen in Fig. 8(C).

Fig. 9(A) shows the time dependence of the integrated area of the bands due to the acrylate species in the 1245–1200 cm^{-1} region formed on Pt/Al_2O_3 with D_{Pt} = 0.21 at 100–200 °C. It appears that not only apparent initial formation rate of the acrylate species but also its apparent consumption rate increased with increasing the reaction temperature. Fig. 9(B) shows the MS profiles of CO_2 as a product, normalized by Ar obtained during the reaction at 100–200 °C. In accordance with the apparent consumption rate of the acrylate species, the initial rate for the formation of CO_2 increased with the reaction temperature. These results suggest that acrylate species participates as a reaction intermediate in C_3H_6 oxidation on Pt/Al_2O_3. As can be seen in Fig. 9(B), the amount of CO_2 formation increased in the first 100 s at 200 °C and then decreased with time on stream. The behavior of CO_2 formation as a function of reaction time is in good agreement with that of acrylate species as seen in Fig. 9(A). Therefore, the formation of acrylate species would be a slow step in the reaction on Pt/Al_2O_3 with D_{Pt} = 0.21 at 200 °C.

Fig. 10 shows the effect of Pt dispersion on the change in the integrated area of the IR bands caused by the acrylate species (1245–1200 cm^{-1}) and the MS profiles of CO_2 normalized by Ar as a function of reaction time over Pt/Al_2O_3 with D_{Pt} = 0.59, 0.21 and 0.07 at 200 °C. Obviously, the apparent initial rates for the formation of acrylate species are very similar irrespective of Pt dispersion. On the other hand, the apparent consumption rate of the acrylate species was found to be very low on Pt/Al_2O_3 with D_{Pt} = 0.07. As can be seen in Fig. 10(B), the amount of CO_2 formation on Pt/Al_2O_3 with D_{Pt} = 0.07 was very low compared with that on other catalysts, although the formation of acrylate species was

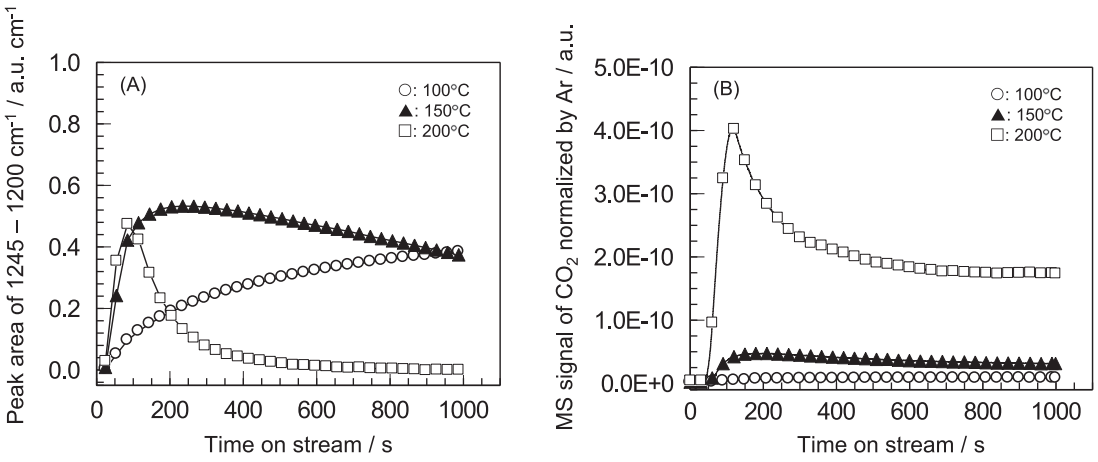

Fig. 9. Time dependence of (A) the integrated area of the bands due to acrylate species in the region of 1245–1200 cm^{-1} formed and (B) MS profiles of CO_2 normalized by Ar taken during C_3H_6 oxidation over Pt/Al_2O_3 with D_{Pt} = 0.21 at 100 (○), 150 (▲) and 200 °C (□). The reaction conditions are the same as these for Fig. 8.

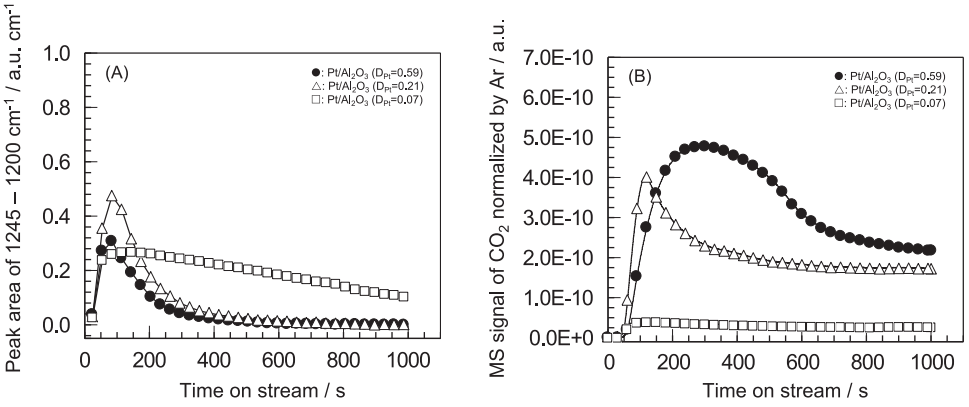

Fig. 10. Time dependence of (A) the integrated area of the bands due to acrylate species in the region of 1245–1200 cm^{-1} formed and (B) MS profiles of CO_2 normalized by Ar taken during C_3H_6 oxidation over Pt/Al_2O_3 with D_{Pt} = 0.59 (●), D_{Pt} = 0.21 (△) and D_{Pt} = 0.07 (□) at 200 °C. The reaction conditions are the same as these for Fig. 8.

clearly observed. These results suggest that the reaction of acrylate species is the slow step in the reaction over Pt/Al_2O_3 with D_{Pt} = 0.07. On the other hand, as described above, the reaction of acrylate species with O_2 to form CO_2 over Pt/Al_2O_3 with D_{Pt} = 0.59 and 0.21 is fast enough.

We have recently reported that the acrylate species formed during the hydrocarbon oxidation over Pt sites would be adsorbed on the appropriate acid–base centers of Al_2O_3 support, which is present at the boundary with Pt particles, *via* the migration from Pt sites, and then react with O_2 on Pt sites [28]. This suggests the possibility that the perimeter interface of Pt particles interacting with Al_2O_3 is catalytically active sites for C_3H_6 oxidation. It is reasonable to understand that the number of perimeter interface of Pt particles decreases with decreasing Pt dispersion. *In situ* FT-IR spectroscopy revealed that C_3H_6 oxidation takes place *via* the formation of acrylate species and that the reaction of the acrylate species on Pt/Al_2O_3 with low Pt dispersion is the slow step. Therefore, the acrylate species are suspected to be accumulated on the perimeter interface of Pt particles, resulting in the inhibition of C_3H_6 oxidation. Poisoning of active sites by acrylate species would be related to a decrease in the TOF of C_3H_6 oxidation on Pt/Al_2O_3 with low Pt dispersion (Fig. 7). On the other hand, the acrylate species formed on the perimeter interface of Pt particles can readily react with oxygen to form CO_2 over Pt/Al_2O_3 with higher Pt dispersion. This is in agreement with the result that the TOF values of C_3H_6 oxidation remained almost invariable above D_{Pt} = 0.20 (Fig. 7).

4. Conclusions

Pt/Al_2O_3 with Pt dispersion ranging from 0.81 to 0.07 estimated by CO chemisorption was prepared. CO conversion to CO_2 on Pt/Al_2O_3 was found to monotonously increase with increasing Pt dispersion. The intrinsic activity, expressed in terms of TOF, for CO oxidation was almost identical irrespective of Pt dispersion, suggesting "structure–insensitive reaction". FT-IR spectroscopy following CO adsorption revealed that the surface electronic state of Pt particles is almost the same irrespective of Pt dispersion. The steady TOF was explained by the identical surface electronic state of Pt particles as catalytically active sites.

Although C_3H_6 conversion to CO_2 over Pt/Al_2O_3 also increased with increasing Pt dispersion, the TOF was found to be strongly dependent on the Pt dispersion. The TOF values increased with increasing the Pt dispersion to 0.20, and then remained almost invariable above D_{Pt} = 0.20, suggesting "structure–sensitive reaction". The formation of acrylate species was observed at the initial stage of the C_3H_6 oxidation reaction over Pt/Al_2O_3 in the FT-IR spectra. The apparent rates for the formation and consumption of the acrylate species increased with the reaction temperature. From the comparison of the consumption of acrylate species and the CO_2 formation, the formation of acrylate species was suspected to be a slow step in the reaction on Pt/Al_2O_3 with higher Pt dispersion, while the reaction of acrylate species being the slow step over Pt/Al_2O_3 with low Pt dispersion. Low TOF values on Pt/Al_2O_3 with

lower Pt dispersion were considered to be due to the inhibition of catalytically active site by accumulation of acrylate species.

Acknowledgements

A part of this work has been supported by a project of the New Energy and Industrial Technology Development Organization (NEDO) under the sponsorship of Ministry of Economy, Trade and Industry (METI) of Japan: “Rare Metal Substitute Materials Development Project”.

References

[1] S. Matsumoto, Catalysis Today 90 (2004) 183–190.
[2] H.C. Yao, Y.F. Yu Yao, Journal of Catalysis 86 (1984) 254–265.
[3] D. Ciuparu, M.R. Lyubovsky, E. Altman, L.D. Pfefferle, A. Datye, Catalysis Reviews 44 (2002) 593–649.
[4] L.M.T. Simplício, S.T. Brandão, D. Domingos, F. Bozon-Verduraz, E.A. Sales, Applied Catalysis A: General 360 (2009) 2–7.
[5] J.R. Rostrup Nielsen, Catalysis Today 18 (1993) 125–145.
[6] H. Yasuda, T. Sato, Y. Yoshimura, Catalysis Today 50 (1999) 63–71.
[7] L. McEwan, M. Julius, S. Reberts, J.C.Q. Fletcher, Gold Bulletin 43 (2010) 298–306.
[8] M. Haruta, Chemical Record 3 (2003) 75–87.
[9] A.K. Prashar, S. Mayadevi, P.R. Rajamohanan, R.N. Devi, Applied Catalysis A: General 403 (2011) 91–97.
[10] H.S. Gandhi, M. Shelef, A. Crucq, A. Frennet (Eds.), Catalysis and Automotive Pollution Control, Elsevier, Amsterdam, 1987, p. 199.
[11] A.M. Gololobov, I.E. Bekk, G.O. Bragina, V.I. Zaikovskii, A.B. Ayupov, N.S. Telegina, V.I. Bukhtiyarov, A. Yu Stakheev, Kinetics and Catalysis 50 (2009) 830–836.
[12] H. Matsuhashi, S. Nishiyama, H. Miura, K. Eguchi, K. Hasegawa, Y. Iizuka, A. Igarashi, N. Katada, J. Kobayashi, T. Kubota, T. Mori, K. Nakai, N. Okazaki, M. Sugioka, T. Umeki, Y. Yazawa, D. Lu, Applied Catalysis A: General 272 (2004) 329–338.
[13] J.A. Anderson, R.A. Daley, S.Y. Christou, A.M. Efstathiou, Applied Catalysis B: Environmental 64 (2006) 189–200.
[14] J.L. Freysz, J. Saussey, J.C. Lavalley, B. Bourges, Journal of Catalysis 197 (2001) 131–138.
[15] B.A. Riguetto, S. Damyanova, G. Gouliev, C.M.P. Marques, L. Petrov, J.M.C. Bueno, Journal of Physical Chemistry B 108 (2004) 5349–5358.
[16] O.S. Alexeev, S.Y. Chin, M.H. Engelhard, L. Ortiz-Soto, M.D. Amiridis, Journal of Physical Chemistry B 109 (2005) 23430–23443.
[17] R.G. Greenler, R.K. Brandt, Colloids and Surfaces A: Physicochemical and Engineering Aspects 105 (1995) 19–26.
[18] P. Hollins, Surface Science Reports 16 (1992) 51–94.
[19] R.G. Greenler, K.D. Burch, K. Kretzschmar, R. Klauser, A.M. Bradshaw, B.E. Hayden, Surface Science 152–153 (1985) 338–345.
[20] F. Coloma, J.M. Coronado, C.H. Rochester, J.A. Anderson, Catalysis Letters 51 (1998) 155–162.
[21] T.F. Garetto, C.R. Apesteguía, Catalysis Today 62 (2000) 189–199.
[22] D.P. Chzhu, P.G. Tsyrul’nikov, E.N. Kudrya, M.D. Smolikov, V.F. Borbat, A.V. Bubnov, Kinetics and Catalysis 43 (2002) 379–383.
[23] D.P. Chzhu, P.G. Tsyrul’nikov, G.N. Kryukova, V.F. Borbat, E.N. Kudrya, M.D. Smolikov, A.V. Bubnov, Kinetics and Catalysis 45 (2004) 406–413.
[24] P. Marécot, A. Fakche, B. Kellali, G. Mabilon, M. Prigent, J. Barbier, Applied Catalysis B: Environmental 3 (1994) 283–294.
[25] L.M. Carballo, E.E. Wolf, Journal of Catalysis 53 (1978) 366–373.
[26] Y.F. Yu Yao, Journal of Catalysis 87 (1984) 152–162.
[27] M. Haneda, M. Sasaki, H. Hamada, M. Ozawa, Topics in Catalysis 56 (2013) 249–254.
[28] M. Haneda, M. Sasaki, H. Hamada, M. Ozawa, Catalysis Letters 141 (2011) 1262–1267.
[29] A.A. Davydov, in: C.H. Rochester (Ed.), Infrared Spectroscopy of Adsorbed Species on the Surface of Transition Metal Oxides, Wiley, Chichester, 1990.
[30] J.A. Anderson, C.H. Rochester, Journal of Chemical Society Faraday Transactions 1: Physical Chemistry in Condensed Phases 85 (1989) 1117–1128.
[31] A. Iglesias-Juez, A.B. Hungría, A. Martínez-Arias, A. Fuerte, M. Fernández-García, J.A. Anderson, J.C. Conesa, J. Soria, Journal of Catalysis 217 (2003) 310–323.
[32] C. Chauvin, J. Saussey, J.C. Lavalley, H. Idriss, J. Hindermann, A. Kiennemann, P. Chaumette, P. Courty, Journal of Catalysis 121 (1990) 56–59.
[33] E. Finocchio, M. Daturi, C. Binet, J.C. Lavalley, G. Blanchard, Catalysis Today 52 (1999) 53–63.